IJSM International Journal of Secondary Metabolite

International Journal of Secondary Metabolite
2022, Vol. 9, No. 3, 305–319

https://doi.org/10.21448/ijsm.1052662

Published at https://dergipark.org.tr/en/pub/ijsm **Research Article**

An application of $CoFe_2O_4$/alginate magnetic beads: drug delivery system of 5-fluorouracil

Aysegul Yildirim[1], **Yasemin Ispirli Dogac**[2,*]

[1]Muğla Sıtkı Koçman University, Graduate School of Natural and Applied Sciences, Department of Molecular Biology and Genetics, Muğla, Türkiye
[2]Muğla Sıtkı Koçman University, Muğla Vocational School, Department of Chemistry and Chemical Processing Technology, Muğla, Türkiye

Abstract: Magnetic hyperthermia therapy is expected to play an important role in the treatment of more and more cancers. The synergistic effects of using together hyperthermia and cancer drugs have been shown by literature studies to be more effective than either hyperthermia treatment alone or chemotherapy alone. In addition, magnetic materials that can be used as a contrast agent enable magnetic resonance imaging of the tumor, which is also useful in seeing the treatment progress. This study, which was designed for this purpose, occurred in three parts: In the first part, magnetic $CoFe_2O_4$/alginate composite beads were prepared and characterized with thermogravimetric analysis (TGA) and scanning electron microscope (SEM). In the second part, the swelling behaviour of magnetic composite beads was investigated at pH 1.2, pH 7.4 and pH 6.8. It was seen that at pH 7.4 and pH 6.8, that is, near neutral pH, CFA swelled by 81.54% and 82.69%, respectively. In the third part, 5-Fluorouracil was encapsulated at the different ratios in $CoFe_2O_4$/alginate composite beads, and release experiments were performed at pH 1.2, pH 7.4 and pH 6.8. 5-FU release was calculated with Korsmeyer-Peppas, Higuchi, first-order, and zero-order models. It was seen that the drug release systems prepared were suitable for all kinetic models. Magnetic $CoFe_2O_4$/alginate composite bead, which is the drug carrier, was determined to be suitable for controlled release for 5-Fluorouracil.

ARTICLE HISTORY
Received: Jan. 03, 2022
Revised: May 09, 2022
Accepted: July 31, 2022

KEYWORDS
Drug release,
Cancer drug,
Polymer,
Magnetic particles,
Hyperthermia

1. INTRODUCTION

A polymeric bead is a type of hydrogel. It has porous with high surface area and hydrated molecular structure. A bead network is formed by chemical or physical crosslinking (Chang & Zhang, 2011). Due to the hydrated molecular structure, beads can absorb water and swell several times under appropriate physiological conditions (Yadollahi *et al.*, 2014). Because of these features, they can stimulate the biological and physicochemical properties of the tissue microenvironment (Gaharwar *et al.*, 2014). Many studies have involved the investigation of alginate beads usage: Alginate has been used for encapsulation of chemical and biological compounds with a wide range of applications in pharmaceutical cosmetics, drug delivery, agriculture, chemical engineering, food technologies, environmental engineering, textile

*CONTACT: Yasemin Ispirli Dogac y-ispirli@hotmail.com Muğla Sıtkı Koçman University, Muğla Vocational School, Department of Chemistry and Chemical Processing Technology, Muğla, Türkiye

ISSN-e: 2148-6905 / **© IJSM 2022**

industry, and many other areas (Wan *et al.*, 2011; Yagub *et al.*, 2014; Fomina & Gadd, 2014; Doğaç *et al.*, 2015; Wang *et al.*, 2018; Doğaç & Teke, 2021). Why is it preferred for so many applications? Alginate is an anionic polysaccharide and has many abilities such as water-solubility, high viscosity, hydrophilicity, pH sensitivity, biocompatibility, biodegradability, transparency, non-toxic and good forming ability. The sodium alginate solution can act as an irreversible chemical reaction with many polyvalent cations to form a crosslinking structure. So, when Ca^{2+} is added to the sodium alginate solution, a Ca^{2+} replaces two Na^{+} to form a calcium alginate structure (Doğaç *et al*., 2015; Wang *et al.*, 2019; Doğaç & Teke, 2021).

The use of magnetic polymeric materials is an innovative technology. The aim here is to add a magnetic property to the polymeric material in addition to its other properties. Generally, spinel ferrites are used when designing magnetic polymeric materials. Spinel ferrites are of interest in the field of medical diagnostics and therapy, enzyme immobilization, RNA/DNA purification, drug delivery systems, biosensors, immunosensors, information storage systems, microwave absorbers, magnetic fluids, and magnetic bulk cores (Kumar & Mohammad, 2011; Huang *et al.*, 2012; Fan *et al.*, 2017; Gong *et al.*, 2017; Luo *et al.*, 2017). The cubic-spinel structure of transition-metal oxides such as XFe_2O_4 (X=Ni, Mn, Co, Zn, Mg, Cu or Fe, etc.) is Fe^{3+} occupies the tetrahedral sites and X^{2+} resides in the octahedral interstitial sites of the close-packed O^{2-} ions (Köseoğlu, 2013; Doğaç *et al.*, 2015; Ramakrishna *et al.*, 2017; Lal *et al.*, 2020; Dhiman *et al.*, 2020; Wang *et al.*, 2018; Doğaç & Teke, 2021).

Today, the production of various materials and the evaluation of the usability of these materials in different applications are among the research that has been given a lot of attention. The synthesis of different magnetic materials and their optimization and application for different areas is one of the important topics in this field. It is thought that examining these materials, which researchers have been seriously interested in especially for the last ten years, on biomaterial production will contribute to the literature.

Magnetic hyperthermia therapy is expected to play an important role in the treatment of more and more cancers. The synergistic effects of using together with hyperthermia and cancer drugs have been shown by literature studies to be more effective than either hyperthermia treatment alone or chemotherapy alone. In addition, magnetic materials that can be used as a contrast agent enable magnetic resonance imaging of the tumor, which is also useful in terms of seeing the progress of the treatment (Ito *et al*., 2003; Prasad *et al.*, 2007; Kumar & Mohammad, 2011; Lartigue *et al.*, 2013; Arami *et al.*, 2015; Ganguly & Margel, 2021).

Various magnetic carriers used for drug release systems were presented in the previous studies (Osterrieth & Fairen-Jimenez, 2021; Ribeiro *et al*., 2021; Zhao *et al*., 2021; Zhalechin *et al*., 2021; Salmanian *et al*., 2021). Magnetic carriers such as Fe_3O_4/ Polyvinyl alcohol, Fe_3O_4/ silica, Fe_3O_4/ poly (ε-caprolactone), Salecan-g-PCH/Fe_3O_4/SiO_2 loaded with a cancer drug Doxorubicin have been reported as drug release system (Kayal & Ramanujan, 2010; Chen *et al*., 2010; Wang *et al*., 2018; Hu *et al*., 2018). Alginate/Fe_3O_4 microspheres, chitosan/alginate/Fe_3O_4 hydrogels, alginate/gelatine/Fe_3O_4 hydrogels, cellulose/Fe_3O_4 bionanocomposites, casein/folic acid/Fe_3O_4, chitosan/Fe_3O_4 nanoparticles, cyclodextrin/poly(methylmethacrylate)/$SmFeO_3$, chitosan/polyacrylic acid/Fe_3O_4 hydrogels, etc. magnetic carriers have been applied for drug delivery of 5-Fluorouracil (Wang *et al.*, 2009; Wang *et al.*, 2017; Anirudhan & Christa, 2018; Chen *et al.*, 2019; Amini-Fazl & Mohammadi, 2019; Hariharan *et al.*, 2019; Jahanban-Esfahlan *et al.*, 2020; Yusefi *et al.*, 2021). Fe_3O_4 was used as a magnetic particle in most of these studies, and studies on other magnetic particles are less common. Therefore, this present study with different magnetic particles ($CoFe_2O_4$) will make a successful contribution to the literature.

In this study, 5-Fluorouracil (5-FU), which is commonly used as a drug for many types of cancer was encapsulated with magnetic $CoFe_2O_4$/alginate beads to create a controlled drug

system. This study includes characterization of the magnetic $CoFe_2O_4$/alginate beads, the swelling character of the release system and release kinetics. The success of the release system for many types of cancer cell cultures is still being investigated.

2. MATERIAL and METHODS

2.1. Materials

Disodium hydrogen phosphate, acetic acid, sodium citrate dihydrate, Tris, HCl, ethanol, cobalt (II) chloride, iron (III) sulfate monohydrate, sodium alginate from Sigma Chemical, sodium hydroxide, citric acid monohydrate from Merck Chemical and 5-Fluorouracil (5-FU) (500mg/10mL) from Koçak Farma were purchased.

2.2. Synthesis of Cobalt Ferrite ($CoFe_2O_4$) Magnetic Nanoparticles

$CoFe_2O_4$ magnetic nanoparticles were synthesized by co-precipitating Fe^{3+} and Co^{2+} ions (Reddy *et al.*, 2015). First, 100 mL of 0.4 M Fe^{3+} solution and 100 mL 0.2 M Co^{2+} solution were mixed. Until the pH 12, 3 M NaOH solution was added dropwise to this mixture. The resulting solution was incubated at 80ºC for half an hour. After that, it was cooled to room temperature. Then the solution was centrifuged at 1500 rpm for 30 minutes. The $CoFe_2O_4$ particles were washed 3 times with distilled water and then left to dry in an oven at 60ºC for 1 week.

2.3. Preparation of Cobalt Ferrite/Alginate (CFA) Magnetic Beads

First, 1% or 2% (w/v) alginate solution was prepared by dissolving in distilled water. Different amounts (25, 50, 75 or 100 mg) of magnetic particles ($CoFe_2O_4$) were homogeneously dispersed in the alginate solution by ultrasonication for 30 minutes at room temperature. While the prepared 2% (w/v) $CaCl_2$ solution was mixed in the magnetic stirrer, the $CoFe_2O_4$ particles/alginate mixture was added dropwise with an injector and the formed beads were incubated in this solution for 1 day. These formed beads were washed 3 times in distilled water after 1 day.

2.4. Characterization of CFA Magnetic Beads

Thermal analysis of raw $CoFe_2O_4$ nanoparticles and CFA magnetic beads obtained under different conditions were performed using Perkin Elmer TGA 4000 (thermo-gravimetric analyser at a constant heating rate of 20º C/min at 30–650 º C under N_2 atmosphere. Dried samples in the 4-5 mg range were used for TGA analysis**.** The surface morphology of CFA beads was studied by scanning electron microscopy (SEM) using JEOL JSM 7600 F model (JEOL, Akishima, Japan). SEM samples are coated with a thin layer of gold-palladium.

2.5. 5-Fluorouracil (5-FU) Encapsulation with CFA Magnetic Beads

A 2% (w/v) alginate solution was prepared to form 5-FU loaded CFA beads. 25 mg of $CoFe_2O_4$ magnetic particles nanoparticles were homogeneously dispersed in the alginate solution. The volume fraction of 5-FU in beads has been changed to 1/2, 1/4, 1/6 and 1/8. While the 2% (w/v) $CaCl_2$ solution was mixed in the magnetic stirrer, a dropwise drop of $CoFe_2O_4$ particles/alginate/5-FU mixture was added to the $CaCl_2$ solution. The formed beads were incubated in this solution for 2 hours. Then, the magnetic beads were washed three times with distilled water.

2.6. Swelling Studies of 5-FU Encapsulated CFA Beads

Swelling rates of the synthesized 5-FU encapsulated CFA beads were investigated separately for pH 7.4, pH 6.8 and pH 1.2 media used in drug release experiments. Approximately 0.05 g of dried beads were immersed in 50 mL of buffer solution (pH 7.4, pH 6.8 or pH 1.2) and incubated at room temperature for 5 hours to reach swelling equilibrium. At regular intervals

for 5 hours, the beads were removed from the buffer solution and reweighed. All experiments were performed with three repetitions. The swelling ratio was calculated using Equation 1.

$$SR\% = [(W_t - W_d)/W_s]x100 \quad \text{(Equation 1)}$$

SR%, swelling rate %; W_t, the mass of the beads at any time t; W_d, dry mass of beads; W_s, the mass of beads after swelling

2.7. Drug Delivery Experiments of 5-FU encapsulated CFA beads

Drug delivery studies of 5-FU encapsulated CFA beads were performed in a 37ºC water bath. It was conducted separately at pH 1.2, 6.8 and 7.4 to examine the drug delivery in the stomach, intestine and blood pH environment. 5-FU loaded CFA beads are placed in falcon tubes and in phosphate buffer solution for certain periods (30. Minutes, 60. Minutes, 90. Minutes, 120. Minutes, 150. Minutes, 180. Minutes, 4. Hours, 5. Hours, 6. Hour, 9. Hour, 12. Hour, 24. Hour) 2000 µl of the sample was taken and 2000 µl of fresh buffer solution was added instead. To understand the drug delivery profiles, the absorbance values of the samples were measured at 266 nm wavelength using a UV spectrophotometer (Thermo Scientific Multiscan GO, Japan). All experiments were performed with three repetitions. Korsmeyer-Peppas (Equation 2), Higuchi (Equation 3), first-order (Equation 4) and zero-order models (Equation 5) were used for mathematical modeling of drug delivery.

$$F = (Q_t/Q) = K_m . t^n \quad \text{(Equation 2)}$$

F, Fraction of drug released at time t; Q_t, amount of drug released at time t; Q, the total amount of drug in a dosage form; K_m, kinetic constant; n, release exponent; t, time in hours.

$$F = A\sqrt{D(2C - Cs)Cs.t} \quad \text{(Equation 3)}$$

F, Fraction of drug released at time t; A, carrier surface area; D, drug diffusion coefficient in the carrier; C, initial drug concentration in the carrier; Cs, the solubility of the drug in the carrier; t, time in hours.

$$\log C = \log C_0 - K.\ t/2{,}303 \quad \text{(Equation 4)}$$

C, drug concentration at time t; C_0, initial drug concentration; K, first-order rate constant; t, time in hours.

$$Q_t = Q_0 + K_0.\ t \quad \text{(Equation 5)}$$

Q_t, amount of drug released at time t; Q_0, the initial amount of drug; K_0, zero-order rate constant; t, time in hours.

3. RESULTS and DISCUSSION

3.1. Optimization of CFA Magnetic Composites

To synthesize CFA magnetic beads, firstly $CoFe_2O_4$ magnetic nanoparticles were formed by the co-precipitation method in an alkali medium. Then, the $CoFe_2O_4$ particle/alginate mixture was injected dropwise into the $CaCl_2$ solution for the crosslinking reaction. Thus, $CoFe_2O_4$ particle/alginate beads were prepared. Hydrogen bonds from the –OH group of magnetic particles and also $-COO^-$ groups in alginate provide the colloidal stability and formation of the core-shell structure which is specific to magnetic composites (Doğaç & Teke, 2021). The high adsorption ability of magnetic polymer occurs due to chelation between $CoFe_2O_4$ particles and alginate.

Optimization parameters of CFA magnetic beads prepared in this study were determined as 1.5-2 % alginate concentration, 25-100 mg magnetic $CoFe_2O_4$ particle amount. To define the optimum parameters, CFA magnetic beads that provided the formation of equal-sized beads

were defined as positive due to the absence of tail formation. Also, in some values, no bead formation occurred due to the high viscosity of the $CoFe_2O_4$ /alginate mixture. Evaluation is given in Table 1. So, 2% alginate concentration, 25 mg and 50 mg $CoFe_2O_4$ amounts were used in the next experiments.

Table 1. Preparation parameters and evaluation of CFA magnetic beads.

Sample name	Alginate Concentration (%)(w/v)	$CoFe_2O_4$ Amount (mg/mL)	Evaluation
CFA-25-1.5	% 1.5	25	*
CFA-50-1.5	% 1.5	50	*
CFA-75-1.5	% 1.5	75	*
CFA-100-1.5	% 1.5	100	*
CFA-25-2	% 2	25	+
CFA-50-2	% 2	50	+
CFA-75-2	% 2	75	**
CFA-100-2	% 2	100	**

Evaluation: Examples were named with abbreviations. CFA was used as an abbreviation for cobalt ferrite-alginate composite; 25, 50, 75 and 100 indicated mg amount of cobalt ferrite; 1.5 and 2 showed alginate concentration. During examining the parameters, CFA beads that provided the formation of equal-sized beads were defined as positive (+).
* These beads were not used as tails occur.
** No beads were formed because of the high viscosity.

3.2. Characterization of CFA magnetic beads

3.2.1. *TGA experiments*

After the evaluation depending on different parameters (Table 1), TGA experiments were made for crude $CoFe_2O_4$ (CF) and two different samples (CFA-25-2 and CFA-50-2) which were prepared with 2% alginate concentration and 25-50 mg $CoFe_2O_4$ particles amount. The experiments were applied with a Perkin Elmer TGA 4000 thermogravimetric analyser between 30-650ºC at a constant heating rate of 20ºC/min. The TGA results are given in Figure 1.

Figure 1. TGA curves of crude $CoFe_2O_4$ particles (CF) and CFA.

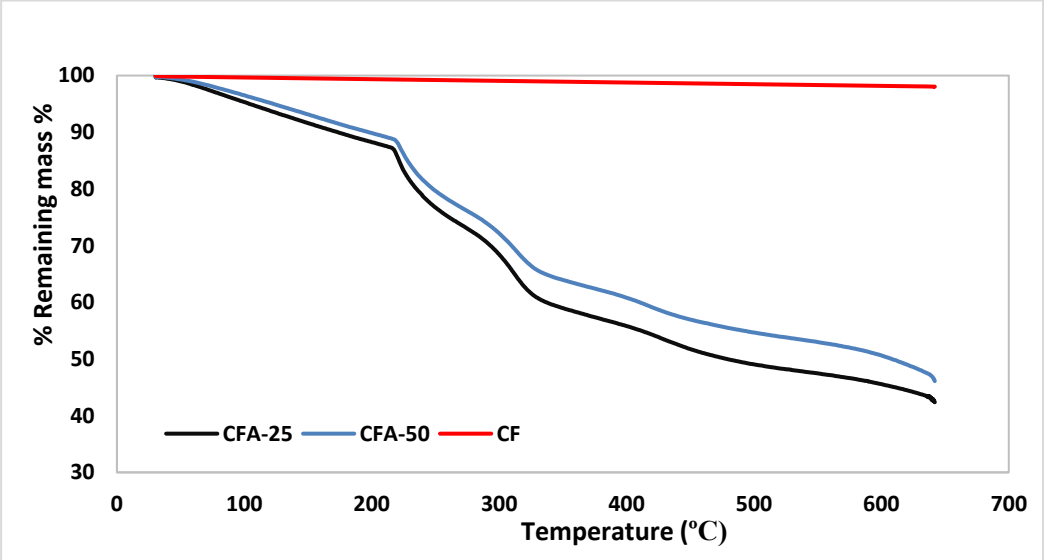

Two-step degradation took place in the samples. As the temperature increased, the mass loss gradually increased and the first sharp decay stages took place after 220 °C. This is due to the release of water which is tightly bound via polar interactions with the carboxylate groups of the alginate and the decomposition of the cyclic products, followed by the loss of CO_2 from the polysaccharide (alginate). In thermogravimetric results of magnetic composites, when the polymer part is entirely burned at certain temperatures, significant combustion does not occur in magnetic particles due to their structure. The lack of significant mass loss (~2 %) in the raw $CoFe_2O_4$ particle sample supports this situation. For this reason, it can be said that the remaining mass as a result of the analysis shows the magnetic particle ratio. By the curves in Figure 1, the $CoFe_2O_4$/alginate ratios of the beads were calculated. The results are given in Table 2. So, it was observed that the composites consisted of approximately 50% (44.34% and 48.08%) $CoFe_2O_4$ magnetic particles. TGA curves and magnetic particle/polymer ratios found in the study are in agreement with the literature. In the study of Amiri *et al*. in 2018 about $CoFe_2O_4$/alginate hydrogels, the composition ratio of the hydrogel was found to be 5% alginate and 95% $CoFe_2O_4$ according to TGA results (Amiri *et al.*, 2018). According to the TGA results, it was observed that there was no significant difference in the ratios of $CoFe_2O_4$ and alginate with the amount of $CoFe_2O_4$ particles of 25 or 50 mg. For this reason, in the other experiments, the amount of $CoFe_2O_4$ was kept constant at 25 mg like an alginate concentration (2%).

Table 2. $CoFe_2O_4$ and alginate ratios of CFAs according to TGA curves.

Sample name	Remaining $CoFe_2O_4$ ratio at TGA curve %	Adjusted $CoFe_2O_4$ rate %	Alginate concentration %
CFA-25	%42.36	%44.34	%55.66
CFA-50	%46.10	%48.08	%51.92

Examples were named with abbreviations. CFA was used as an abbreviation for cobalt ferrite-alginate composite; 25 and 50 indicated mg amount of cobalt ferrite. Both samples were prepared with 2% (w/v) alginate.

3.2.2. *SEM-EDS analysis*

SEM images and EDS spectrum of 5-FU loaded and 5-FU unloaded CFA beads are shown in Figure 2. According to the SEM images, the spherical form of the CFA beads and the morphological roughness of the surface were obvious. It can be said that it has a high surface area depending on the roughness of the surface. In addition, SEM analyses determined that the samples mostly consisted of uniform beads. Also, the observation of 5-FU molecules on the composite surfaces from SEM photographs after 5-FU encapsulation (Figure 2-c) indicated that the drug was dispersed throughout the structure. the EDS spectra (Figure 2-d) showed that O (from alginate and $CoFe_2O_4$), C (from alginate), Fe (from $CoFe_2O_4$), Co (from $CoFe_2O_4$) and so, $CoFe_2O_4$ and alginate formed as a composite structure. In addition, the presence of Na determined in the spectrum is due to sodium alginate and the presence of Ca is due to Ca^{2+}, which provides a bead form by cross-linking the alginate chains. The mean diameters of the beads were in the range of 0.93 to 0.99 mm.

Figure 2. The photograph, SEM images and EDS spectrum of CFA beads (2% alginate and 25 mg $CoFe_2O_4$) (a) and (b) CFA, (c) CFA-5-FU, (d) EDS spectrum of CFA, (e) The photograph of magnetic beads attracted by the magnetic bar.

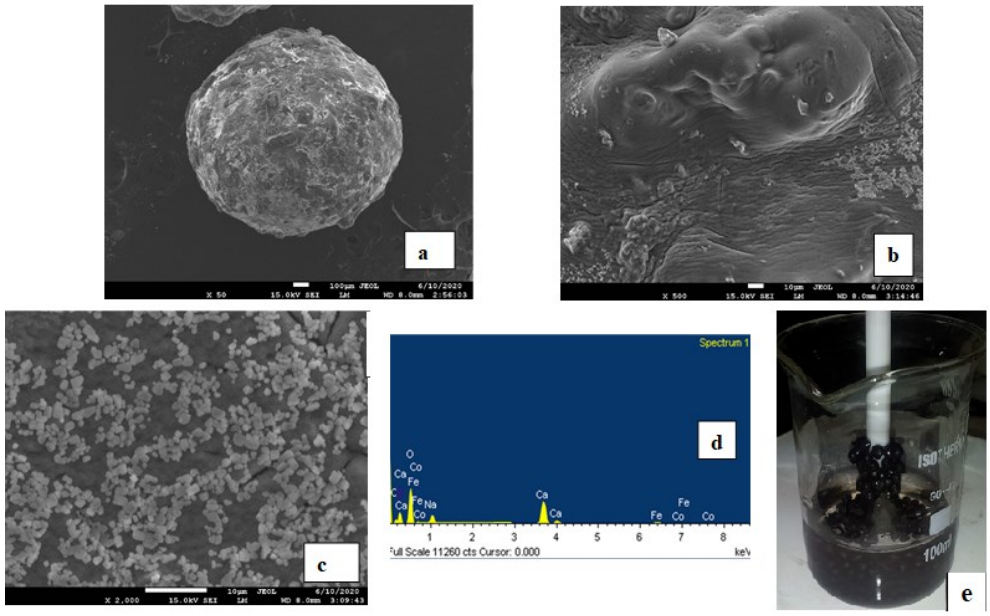

3.3. Determination of Swelling Behaviour of CFA Beads

Swelling rates of the prepared CFA beads were examined separately for pH 1.2, pH 6.8 and pH 7.4 media used in drug release experiments. Swelling curves are given in Figure 3. When Figure 3 was evaluated, it was seen that at pH 7.4 and pH 6.8, that is, near neutral pH, CFA swelled by 81.54% and 82.69%, respectively. They exhibited similar swelling behaviours at these two pHs and the behaviours were quite good. At pH 1.2, that is in an acidic environment, although a decrease in the swelling rate was observed (67.17%), the structures continued to maintain their pH stability. The swelling character of the synthesized CFA beads is due to the polymer in their content, namely alginate. It is thought that the swelling phenomenon is mainly based on the -OH groups in the structure of the alginate, making H bonds with water and also the ionic interactions between the alginate chains themselves support swelling. In the literature, this interaction has been linked to the crosslinker density as it controls the chain mobility and it has been reported that while crosslinking density increases, swelling and sensitivity to pH decrease and the structural stability increases (Dai *et al.*, 2008).

Figure 3. Swelling behaviour profiles of CFA beads at pH 7.4 (a), pH 6.8 (b) and pH 1.2 (c).

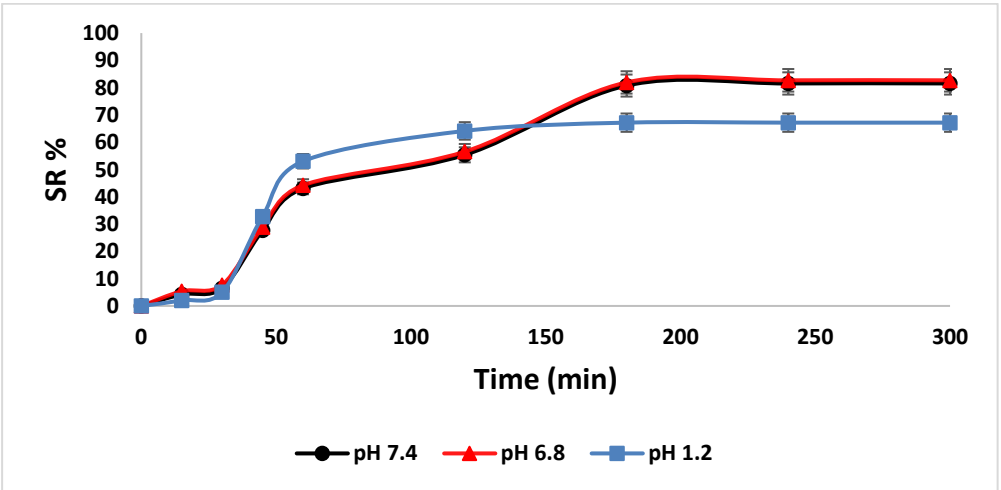

3.4. Release Experiments and Release Kinetics of 5-FU Encapsulated CFA Beads

5-Fluorouracil (5-FU) that is used for the treatment of breast, rectum, colon, stomach, pancreatic cancers and also bladder, cervix, neck, ovarian, liver, skin, and prostate cancers is selected as a model cancer drug during drug release experiments. If it is metabolized in free form, it reaches its maximum grade in plasma after 3 hours. Due to the increase in the drug amount in the blood in a short time, serious side effects occur in the patient. In this study, it was suggested to gradually increase the amount of drug in plasma and tissues by encapsulating 5-FU to CFA and as a result, it was aimed to reduce the side effects that would occur in the patient.

In 5-FU release experiments, the volume fraction of 5-FU in CFA beads was altered as 1/2, 1/4, 1/6, and 1/8 and the release experiments were applied in vitro at pH 7.4 (blood), pH 6.8 (colon-rectum) and pH 1.2 (stomach). Results were calculated based on Korsmeyer-Peppas, Higuchi, first-order and zero-order models. The Korsmeyer-Peppas model is appropriate for controlled drug systems prepared in different geometric shapes such as cylinder, sheet, disk and sphere. It means that the release is not late and there is no immediate release in the drug system (Korsmeyer & Peppas, 1983). The Higuchi model is suitable for slow-release systems that applied the release of randomly dispersed drug molecules in solid or semi-solid carriers with high surface area and high porosity (Higuschi, 1963). The first order model is based on a logarithmic reduction in the amount of unreleased drug over time and is a model that most conventional drug doses and sustained-release systems fit (Kitazawa *et al.*, 1977). The zero-order model indicates that the amount of drug released is constant at each time interval, and especially controlled or extended-release systems are intended to suit this model (Varelas *et al.*, 1995). R^2 values of release systems calculated according to all models are given in Table 3. And also, the curves of the zero-order model of 5-FU encapsulated CFA beads are shown in Figure 4, Figure 5 and Figure 6.

Figure 4. Zero order model of FU release of CFA at pH 7.4.

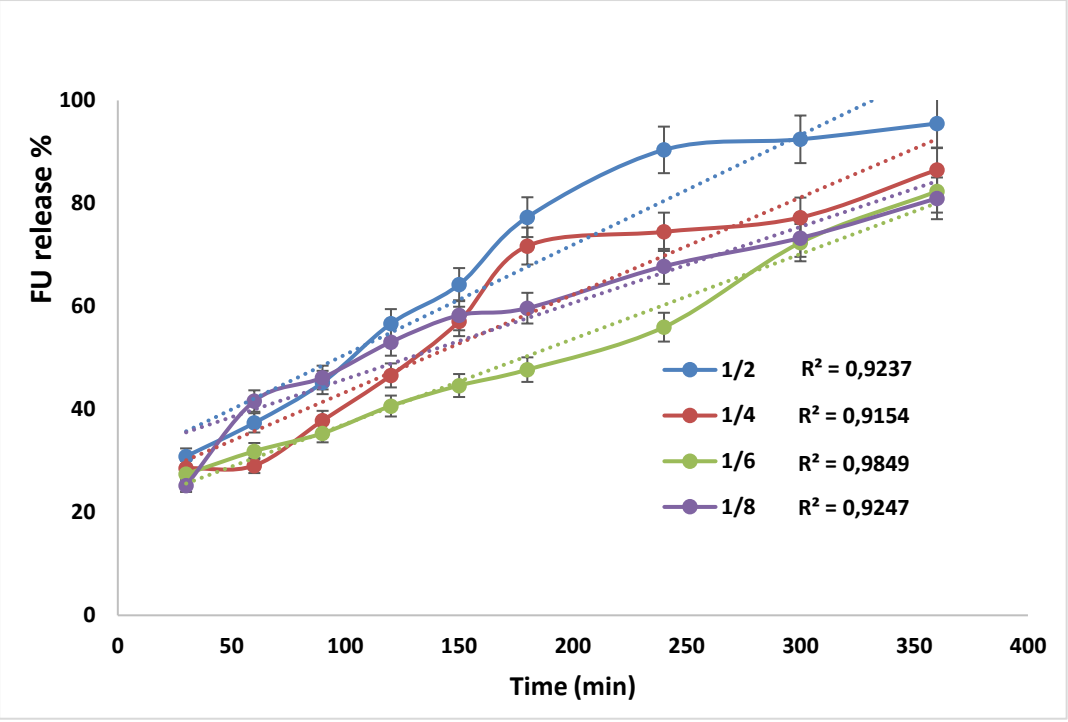

Figure 5. Zero order model of FU release of CFA at pH 6.8.

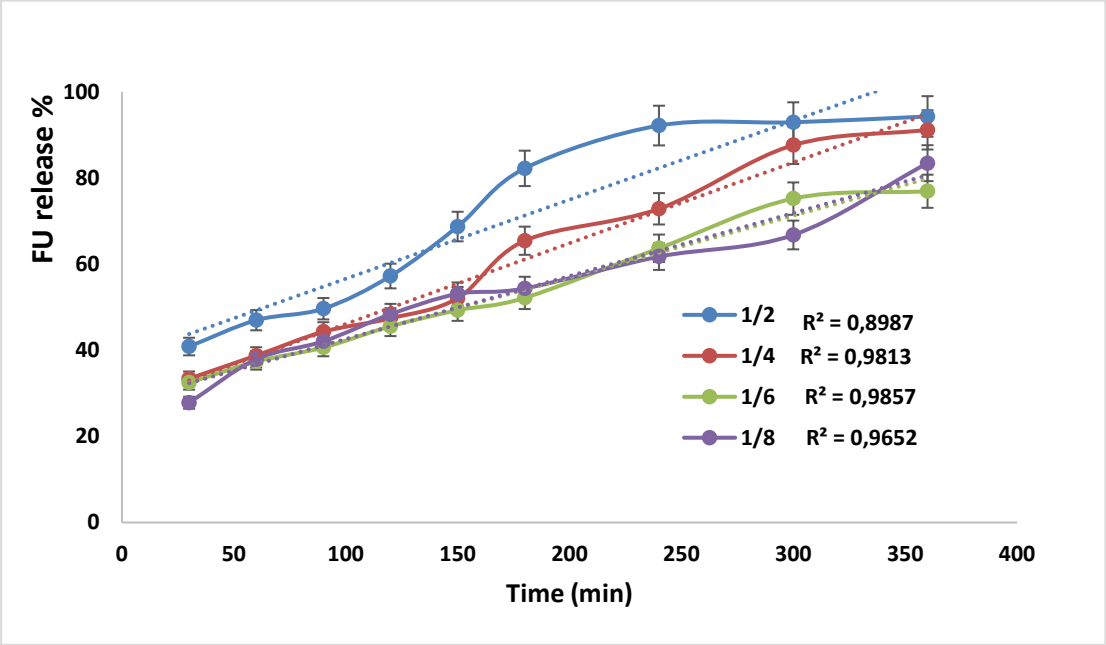

Figure 6. Zero order model of FU release of CFA at pH 1.2.

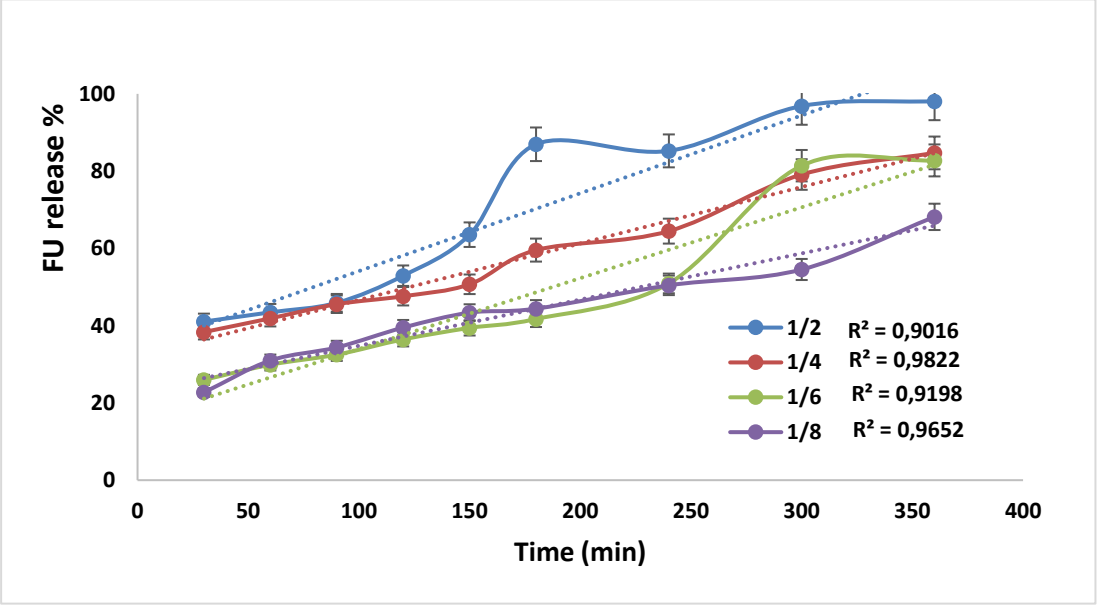

When evaluating the synthesized release systems, R^2 values for all models were calculated and values of 0.9 and above were considered to be suitable for mathematical models. 5-FU encapsulated CFA beads comply with the Korsmeyer-Peppas model, Higuchi model and first-order model at all pH values studied (including pH 1.2, which is a strongly acidic environment), that is carriers consisting of polymeric structures do not delay the release, do not cause immediate release, have high porosity and high surface area, the amount of active substance not released decreased logarithmically over time and it was a controlled drug system. In addition, it is possible to say that the prepared magnetic carrier drug system has succeeded in all drug amounts at the zero order model. So, it was observed that it managed to keep the amount of released active substance constant over time.

When the experiments were evaluated at pH 7.4, pH 6.8 and pH 1.2, a slight relative decrease was observed in the release rate at pH 1.2. This may be attributed to the protonation of exposed carboxylic acid groups present in alginate in an acidic medium (pH 1.2). Protonation of the construct may have caused a decrease in the diffusion of the drug. This result seems to be in parallel with the decrease in swelling ratios obtained in swelling experiments. The high swelling rates obtained at pH 7.4 and 6.8 support the high release rate at these pHs.

The carrier (CFA) used in the present study has two different release studies with a different drug in the literature. CFA was studied for the release of chlorpheniramine maleate in 2017 and it was reported that the release diffusion was faster at pH 7.4 compared to pH 1.2, but R^2 values were not given (Amiri *et al.*, 2017). In this sense, although it was found to be compatible with the pH results found in our study, a comparison could not be made in this direction because the R^2 values were not given in the article. In another study about $CoFe_2O_4$/alginate beads loaded with chlorpheniramine maleate, the release kinetics were determined according to the Korsmeyer-Peppas release model and this model was reported to be suitable (Amiri *et al*., 2018).

Table 3. Regression values of kinetic models of 5-FU encapsulated CFA beads.

Kinetic models	Volumetric ratio of 5-FU	R^2 values		
		pH 7.4	pH 6.8	pH 1.2
Korsmeyer -Peppas model	1/2	0.9692	0.9275	0.9053
	1/4	0.9275	0.9368	0.9086
	1/6	0.9218	0.9389	0.9061
	1/8	0.9743	0.9788	0.9788
Higuchi model	1/2	0.9641	0.9326	0.9079
	1/4	0.9450	0.9589	0.9334
	1/6	0.9323	0.9619	0.9035
	1/8	0.9797	0.9655	0.9655
First order model	1/2	0.9751	0.9401	0.9238
	1/4	0.9587	0.9460	0.9361
	1/6	0.9186	0.9665	0.9027
	1/8	0.9837	0.9079	0.9464
Zero order model	1/2	0.9237	0.9887	0.9016
	1/4	0.9154	0.9813	0.9822
	1/6	0.9849	0.9857	0.9198
	1/8	0.9247	0.9652	0.9652

The magnetic particle and alginate concentrations in all samples were kept constant at 25 mg and 2% (w/v), respectively.

In the literature, different drugs encapsulated different magnetic polymeric systems were applied for controlled drug systems. When these literature data are examined, it was seen that Fe_3O_4 was generally chosen to form composites with polymeric structures (Supramaniam *et al*., 2018, Wang *et al.*, 2018, Pooresmaeil *et al.*, 2020, Soumia *et al.*, 2020). In this case, it is thought that the $CoFe_2O_4$ magnetic particles presented in this study will contribute to the literature. In these studies, it is not a coincidence that most cancer drugs (especially Doxorubicin) are used (Chen *et al.*, 2010, Kayal & Ramanujan, 2010, Hu *et al.*, 2018, Wang *et al.*, 2018).

In particular, many studies have been conducted to benefit from magnetic targeting and hyperthermia, in which magnetic materials are used for cancer treatment. Hyperthermia is a practice that involves sending magnetically targeted magnetic nanoparticles to the tumor cell and then exposing this tumor to an external alternating magnetic field. Under a high frequency alternating magnetic field, the temperature inside the tumor cell increases due to heat generation from magnetic nanoparticles. Increasing temperature and heat shock cause denaturation of proteins and also kill cancer cells as it mediates the activation of the immune system. Apart from that, magnetic hyperthermia-based cancer treatments are more effective in cancer treatment, especially in combination with chemotherapy, due to their synergistic effects. This topic is also among the popular topics of recent years (Ito *et al.*, 2003, Prasad *et al.*, 2007, Laurent *et al.*, 2011, Kumar & Mohammad, 2011). In the present study, magnetic CoFe2O4/alginate beads loaded with 5-Fluorouracil (5-FU), an important drug used in cancer chemotherapy, were selected and a system in which a synergistic effect could be created was designed.

4. CONCLUSION

Magnetic hyperthermia therapy is expected to play an important role in the treatment of more and more cancers. The synergistic effects of using together hyperthermia and cancer drugs have been shown by studies in the related literature to be more effective than either hyperthermia treatment alone or chemotherapy alone. In addition, magnetic materials that can be used as a contrast agent enable magnetic resonance imaging of the tumor, which is also useful in seeing the treatment progress. Therefore, in this study, cobalt ferrite/alginate beads were successfully prepared, optimized and characterized by the magnetic core-shell model. This magnetic material was used as the carrier for 5-FU to create the synergistic effect of the magnetic hyperthermia-cancer drug. Here, 5-FU was chosen as a model, and appropriate data were obtained for a controlled drug release system. It is thought that it will be successful in many different drug systems where the same carrier can be used.

Acknowledgments

The authors would like to thank Dr. Ersin Doğaç from Muğla Sıtkı Koçman University for his help with laboratory work.

Declaration of Conflicting Interests and Ethics

The authors declare no conflict of interest. This research study complies with research and publishing ethics. The scientific and legal responsibility for manuscripts published in IJSM belongs to the authors.

Authorship Contribution Statement

Aysegul Yildirim: Investigation, Analysis. **Yasemin Ispirli Dogac:** Methodology, Investigation, Analysis, Resources, Supervision, Validation and Writing -original manuscript.

Orcid

Aysegul Yildirim http://orcid.org/0000-0001-5664-4030
Yasemin Ispirli Dogac http://orcid.org/0000-0001-8616-0280

REFERENCES

Amini-Fazl, M.S., Mohammadi, R., & Kheiri, K. (2019). 5-Fluorouracil loaded chitosan/polyacrylic acid/Fe_3O_4 magnetic nanocomposite hydrogel as a potential anticancer drug delivery system. *International Journal of Biological Macromolecules*, *132*, 506-513. https://doi.org/10.1016/j.ijbiomac.2019.04.005

Amiri, M., Akbari, A., Ahmadi, M., & Pardakhti, A.M. (2018). Synthesis and in vitro evaluation of a novel magnetic drug delivery system; proecological method for the preparation of

$CoFe_2O_4$ nanostructures. *Journal of Molecular Liquids, 249*, 1151-1160. https://doi.org/10.1016/j.molliq.2017.11.133

Amiri, M., Salavati-Niasari, M., Pardakhty, A., Ahmadi, M., & Akbari, A. (2017). Caffeine: A novel green precursor for synthesis of magnetic $CoFe_2O_4$ nanoparticles and pH-sensitive magnetic alginate beads for drug delivery, *Materials Science and Engineering: C*, *76*, 1085-1093. https://doi.org/10.1016/j.msec.2017.03.208

Anirudhan, T.S., & Christa, J. (2018). pH and magnetic field sensitive folic acid conjugated protein–polyelectrolyte complex for the controlled and targeted delivery of 5-fluorouracil. *Journal of Industrial and Engineering Chemistry*, *57*, 199-207. https://doi.org/10.1016/j.jiec.2017.08.024

Arami, H., Khandhar, A., Liggitt, D., & Krishnan, K.M. (2015). In Vivo Delivery, Pharmacokinetics, biodistribution and toxicity of Iron Oxide nanoparticles. *Chemical Society Reviews*, *44*, 8576−8607. https://doi.org/10.1039/C5CS00541H

Chang, C., & Zhang, L. (2011). Cellulose-based hydrogels: present status and application prospects. *Carbohydrate Polymers*,*84*, 40-53. https://doi.org/10.1016/j.carbpol.2010.12.023

Chen, F.H., Zhang, L.M., Chen, Q.T., Zhang, Y., & Zhang, Z.J. (2010). Synthesis of a novel magnetic drug delivery system composed of doxorubicin-conjugated Fe_3O_4 nanoparticle cores and a PEG-functionalized porous silica shell. *Chemical Communications*, *46*(45), 8633-8635. https://doi.org/10.1039/C0CC02577A

Chen, X., Fan, M., Tan, H., Ren, B., Yuan, G., Jia, Y., & Hu, X. (2019). Magnetic and self-healing chitosan-alginate hydrogel encapsulated gelatin microspheres via covalent cross-linking for drug delivery. *Materials Science and Engineering: C*, *101*, 619-629. https://doi.org/10.1016/j.msec.2019.04.012

Dai, Y., Li, P., Zhang, J., Wang, A., & Wei, Q. (2008). Swelling Characteristics and Drug Delivery Properties of Nifedipine-Loaded pH Sensitive Alginate–Chitosan Hydrogel Beads. *Journal of Biomedical Materials Research Part B: Applied Biomaterials, 86*, 493-500. https://doi.org/10.1002/jbm.b.31046

Dhiman, P., Mehta, T., Kumar, A., Sharma, G., Naushad, M., Ahamad, T., & Mola, G.T. (2020). Mg0. 5NixZn0. 5-xFe2O4 spinel as a sustainable magnetic nano-photocatalyst with dopant driven band shifting and reduced recombination for visible and solar degradation of Reactive Blue-19. *Advanced Powder Technology*, *31*(12), 4585-4597. https://doi.org/10.1016/j.apt.2020.10.010

Doğaç, Y.İ., & Teke, M. (2021). Urease immobilized core–shell magnetic Fe [NiFe]O_4/alginate and Fe_3O_4/alginate composite beads with improved enzymatic stability properties: removal of artificial blood serum urea. *Journal of the Iranian Chemical Society*, *18*(10), 2637-2648, https://doi.org/10.1007/s13738-021-02219-7

Doğaç, Y.İ., Çınar, M., & Teke, M. (2015). Improving of catalase stability properties by encapsulation in alginate/Fe_3O_4 magnetic composite beads for enzymatic removal of H_2O_2. *Preparative Biochemistry & Biotechnology*, *45*(2), 144-157. https://doi.org/10.1080/10826068.2014.907178

Fan, W., Yung, B., Huang, P., & Chen X. (2017). Nanotechnology for multimodal synergistic cancer therapy, *Chemical Reviews*, *117*, 13566-13638. https://doi.org/10.1021/acs.chemrev.7b00258

Fomina, M., & Gadd, G.M. (2014). Biosorption: Current perspectives on concept, definition and application. *Bioresource Technology*, *160*, 3-14. https://doi.org/10.1016/j.biortech.2013.12.102

Gaharwar, A.K., Peppas, N.A. & Khademhosseini, A. (2014). Nanocomposite hydrogels for biomedical applications. *Biotechnology and Bioengineering*, *111*, 441-453. https://doi.org/10.1002/bit.25160

Ganguly, S., & Margel, S. (2021). Design of Magnetic Hydrogels for Hyperthermia and Drug Delivery. *Polymers*, *13*(23), 4259. https://doi.org/10.3390/polym13234259

Gong, L, Yan, L., Zhou, R., Xie, J., Wu, W., & Gu, Z. (2017). Two-dimensional transition metal dichalcogenide nanomaterials for combination cancer therapy, *Journal of Materials Chemistry B*, *5,* 1873-1895. https://doi.org/10.1039/C7TB00195A

Hariharan, M.S., Sivaraj, R., Ponsubha, S., Jagadeesh, R., & Enoch, I.V.M.V. (2019). 5-Fluorouracil-loaded β-cyclodextrin-carrying polymeric poly (methylmethacrylate)-coated samarium ferrite nanoparticles and their anticancer activity. *Journal of Materials Science*, *54*(6), 4942-4951. https://doi.org/10.1007/s10853-018-3161-z

Higuchi T. (1963). Mechanism of sustained-action medication. Theoretical analysis of rate of release of solid drugs dispersed in solid matrices. *Journal of Pharmaceutical Sciences*, *52*(12), 1145-49. https://doi.org/10.1002/jps.2600521210

Hu, X., Wang, Y., Zhang, L., Xu, M., Zhang, J., & Dong, W. (2018). Design of a pH-sensitive magnetic composite hydrogel based on salecan graft copolymer and Fe_3O_4@ SiO_2 nanoparticles as drug carrier. *International Journal of Biological Macromolecules*, *107*, 1811-1820. https://doi.org/10.1016/j.ijbiomac.2017.10.043

Huang, Y., He, S., Cao, W., Cai, K., & Liang, X.J. (2012). Biomedical nanomaterials for imaging-guided cancer therapy, *Nanoscale*, *4*(20), 6135-49. https://doi.org/10.1039/C2NR31715J

Ito, A., Matsuoka, F., Honda, H., & Kobayashi, T. (2003). Heat shock protein 70 gene therapy combined with hyperthermia using magnetic nanoparticles. *Cancer Gene Therapy*, *10*(12), 918-25. https://doi.org/10.1038/sj.cgt.7700648

Jahanban-Esfahlan, R., Derakhshankhah, H., Haghshenas, B., Massoumi, B., Abbasian, M., & Jaymand, M. (2020). A bio-inspired magnetic natural hydrogel containing gelatin and alginate as a drug delivery system for cancer chemotherapy. *International Journal of Biological Macromolecules*, *156*, 438-445. https://doi.org/10.1016/j.ijbiomac.2020.04.074

Kayal, S., & Ramanujan, R.V. (2010). Doxorubicin loaded PVA coated iron oxide nanoparticles for targeted drug delivery. *Materials Science and Engineering: C*, *30*(3), 484-90. https://doi.org/10.1016/j.msec.2010.01.006

Kitazawa, S., Johno, I., Minouchi, T., & Okada, J. (1977). Interpretation of dissolution rate data from in vitro testing of compressed tablets. *Journal of Pharmacy and Pharmacology*, *29*(1), 453-459. https://doi.org/10.1111/j.2042-7158.1977.tb11368.x

Korsmeyer, R.W., & Peppas, N.A. (1983). Controlled release delivery systems. *TJ Roseman and SZ Mansdorf, M. Dekker, New York*, 77-90.

Köseoğlu, Y. (2013). Structural, magnetic, electrical and dielectric properties of MnxNi1−xFe2O4 spinel nanoferrites prepared by PEG assisted hydrothermal method. *Ceramics International*, *39*(4), 4221-4230. https://doi.org/10.1016/j.ceramint.2012.11.004

Kumar C.S.S.R., & Mohammad F., (2011). Magnetic nanomaterials for hyperthermia-based therapy and controlled drug delivery. *Advanced Drug Delivery Reviews*, *63*(9), 789-808. https://doi.org/10.1016/j.addr.2011.03.008

Lal, G., Punia, K., Dolia, S.N., Alvi, P.A., Choudhary, B.L., & Kumar, S. (2020). Structural, cation distribution, optical and magnetic properties of quaternary Co0. 4+ xZn0. 6-xFe2O4 (x= 0.0, 0.1 and 0.2) and Li doped quinary Co0. 4+ xZn0. 5-xLi0. 1Fe2O4 (x= 0.0, 0.05 and 0.1) nanoferrites. *Journal of Alloys and Compounds*, *828*, 154388. https://doi.org/10.1016/j.jallcom.2020.154388

Lartigue, L., Alloyeau, D., Kolosnjaj-Tabi, J., Javed, Y., Guardia, P., Riedinger, A., Pechoux, C., Pellegrino, T., Wilhelm, C., Gazeau, F. (2013). Biodegradation of Iron Oxide nanocubes: High-resolution in situ monitoring. *ACS Nano, 7*, 3939−3952. https://doi.org/10.1021/nn305719y

Laurent, S., Dutz, S., Häfeli U.O., & Mahmoudi, M. (2011) Magnetic fluid hyperthermia: focuson superparamagnetic iron oxide nanoparticles. *Advances in Colloid and Interface science*, *166*, 8-23. https://doi.org/10.1016/j.cis.2011.04.003

Luo, L., Shu, R., & Wu, A., (2017). Nanomaterial-based cancer immunotherapy. *Journal of Materials Chemistry B*, 5, 5517-5531. https://doi.org/10.1016/j.cis.2011.04.003

Osterrieth, J. W., & Fairen-Jimenez, D. (2021). Metal–organic framework composites for theragnostics and drug delivery applications. *Biotechnology Journal*, *16*(2), 2000005. https://doi.org/10.1002/biot.202000005

Pooresmaeil, M., Javanbakht, S., Nia, S.B., & Namazi, H., (2020). Carboxymethyl cellulose/mesoporous magnetic graphene oxide as a safe and sustained ibuprofen delivery bio-system: Synthesis, characterization, and study of drug release kinetic. *Colloids and Surfaces A: Physicochemical and Engineering Aspects*, *594*, 124662. https://doi.org/10.1016/j.colsurfa.2020.124662

Prasad, N.K., Rathinasamy, K., Panda, D., & Bahadur, D., (2007). Mechanism of cell death induced by magnetic hyperthermia with nanoparticles of γ-MnxFe2–xO3 synthesizedby a single step process. *Journal of Materials Chemistry*, *48*, 5042-5051. https://doi.org/10.1039/B708156A

Ramakrishna, K.S., Srinivas, C., Meena, S.S., Tirupanyam, B.V., Bhatt, P., Yusuf, S.M., & Sastry, D.L. (2017). Investigation of cation distribution and magnetocrystalline anisotropy of NixCu0. 1Zn0. 9− xFe$_2$O$_4$ nanoferrites: role of constant mole percent of Cu^{2+} dopant in place of Zn^{2+}. *Ceramics International*, *43*(11), 7984-7991. https://doi.org/10.1016/j.ceramint.2017.03.078

Reddy, M.P., Mohamed, A.M.A., Zhou, X.B., Du, S., & Huang, Q., (2015). A facile hydrothermal synthesis, characterization and magnetic properties of mesoporous CoFe$_2$O$_4$ nanospheres. *Journal of Magnetism and Magnetic Materials*, *388*, 40-4. https://doi.org/10.1016/j.jmmm.2015.04.009

Ribeiro, M., Boudoukhani, M., Belmonte-Reche, E., Genicio, N., Sillankorva, S., Gallo, J., & Bañobre-López, M. (2021). Xanthan-Fe3O4 Nanoparticle Composite Hydrogels for Non-Invasive Magnetic Resonance Imaging and Magnetically Assisted Drug Delivery. *ACS Applied Nano Materials*, *4*(8), 7712-7729. https://doi.org/10.1021/acsanm.1c00932

Salmanian, G., Hassanzadeh-Tabrizi, S.A., & Koupaei, N. (2021). Magnetic chitosan nanocomposites for simultaneous hyperthermia and drug delivery applications: A review. *International Journal of Biological Macromolecules*, *184*,618-635. https://doi.org/10.1016/j.ijbiomac.2021.06.108

Soumia, A., Adel, M., Amina, S., Bouhadjar, B., Amal, D., Farouk, Z., Abdelkader, B., & Mohamed, S., (2020). Fe$_3$O$_4$-alginate nanocomposite hydrogel beads material: One-pot preparation, release kinetics and antibacterial activity. *International Journal of Biological Macromolecules*, *145*, 466-75. https://doi.org/10.1016/j.ijbiomac.2019.12.211

Supramaniam, J., Adnan, R., Kaus, N.H.M., & Bushra, R. (2018). Magnetic nanocellulose alginate hydrogel beads as potential drug delivery system. *International Journal of Biological Macromolecules*,*118*, 640-48. https://doi.org/10.1016/j.ijbiomac.2018.06.043

Varelas, C.G., Dixon, D.G., & Steiner, C. (1995). Zero-order release fromstudies. II. Dissolution of particles under conditions of rapid agitation.biphasic polymer hydrogels. *Journal of Controlled Release*, *34*, 185–192. https://doi.org/10.1016/0168-3659(94)00085-9

Wan Ngah, W.S., Teong, L.C., & Hanafiah, M.A K.M. (2011). Adsorption of dyes and heavy metal ions by chitosan composites: A review. *Carbohydrate Polymers*, *83*(4), 1446–1456. https://doi.org/10.1016/j.carbpol.2010.11.004

Wang, B., Gao, B., Zimmerman, A., & Lee, X. (2018). Impregnation of multiwall carbon nanotubes in alginate beads dramatically enhances their adsorptive ability to aqueous

methylene blue. *Chemical Engineering Research and Design*, *133*, 235-242. https://doi.org/10.1016/j.cherd.2018.03.026

Wang, B., Wan, Y., Zheng, Y., Lee, X., Liu, T., Yu, Z., & Gao, B. (2019). Alginate-based composites for environmental applications: a critical review. *Critical Reviews in Environmental Science and Technology*, *49*(4), 318-356. https://doi.org/10.1080/10643389.2018.1547621

Wang, D.S., Li, J.G., Li, H.P., & Tang, F.Q. (2009). Preparation and drug releasing property of magnetic chitosan-5-fluorouracil nano-particles. *Transactions of Nonferrous Metals Society of China*, *19*(5), 1232-1236. https://doi.org/10.1016/S1003-6326(08)60434-3

Wang, G., Zhao, D., Li, N., Wang, X., & Ma, Y. (2018). Drug-loaded poly (ε-caprolactone)/Fe_3O_4 composite microspheres for magnetic resonance imaging and controlled drug delivery. *Journal of Magnetism and Magnetic Materials*, *456*, 316-23. https://doi.org/10.1016/j.jmmm.2018.02.053

Wang, Q., Liu, S., Yang, F., Gan, L., Yang, X., & Yang, Y. (2017). Magnetic alginate microspheres detected by MRI fabricated using microfluidic technique and release behavior of encapsulated dual drugs. *International Journal of Nanomedicine*, *12*, 4335. https://doi.org/10.2147/IJN.S131249

Yadollahi, M., Namazi, H., & Barkhordari, S. (2014). Preparation and properties of carboxymethyl cellulose/layered double hydroxide bionanocomposite films. *Carbohydrate Polymers*, *108*, 83-90. https://doi.org/10.1016/j.carbpol.2014.03.024

Yagub, M.T., Sen, T.K., Afroze, S., & Ang, H.M. (2014). Dye and its removal from aqueous solution by adsorption: A review. *Advances in Colloid and Interface Science*, *209*, 172–184. https://doi.org/10.1016/j.cis.2014.04.002

Yusefi, M., Lee-Kiun, M.S., Shameli, K., Teow, S.Y., Ali, R.R., Siew, K.K., & Kuča K. (2021). 5-fluorouracil loaded magnetic cellulose bionanocomposites for potential colorectal cancer treatment. *Carbohydrate Polymers*, *273*, 118523. https://doi.org/10.1016/j.carbpol.2021.118523

Zhalechin, M., Dehaghi, S. M., Najafi, M., & Moghimi, A. (2021). Magnetic polymeric core-shell as a carrier for gradual release in-vitro test drug delivery. *Heliyon*, *7*(5), e06652. https://doi.org/10.1016/j.heliyon.2021.e06652

Zhao, K., Gong, P., Huang, J., Huang, Y., Wang, D., Peng, J., & Liu, Z. (2021). Fluorescence turn-off magnetic COF composite as a novel nanocarrier for drug loading and targeted delivery. *Microporous and Mesoporous Materials*, *311*, 110713. https://doi.org/10.1016/j.micromeso.2020.110713